# Monovalent Metal Ions Play an Essential Role in Catalysis and Intersubunit Communication in the Tryptophan Synthase Bienzyme Complex†

Eilika U. Woehl and Michael F. Dunn*

*Department of Biochemistry, University of California at Riverside, Riverside, California 92521-0129*

*Received December 22, 1994; Revised Manuscript Received March 13, 1995*⊗

ABSTRACT: This investigation shows that the $\alpha_2\beta_2$ tryptophan synthase bienzyme complex from *Salmonella typhimurium* is subject to monovalent metal ion activation. The effects of the monovalent metal ions $Na^+$ and $K^+$ were investigated using rapid scanning stopped-flow (RSSF), single-wavelength stopped-flow (SWSF), and steady-state techniques. RSSF measurements of individual steps in the reaction of L-serine and indole to give L-trytophan (the $\beta$-reaction) as well as the reaction of 3-indole-D-glycerol 3′-phosphate (IGP) with L-serine (the $\alpha\beta$-reaction) demonstrate that monovalent metal ions such as $Na^+$ and $K^+$ change the distribution of intermediates in both the transient and steady states. Therefore the metal ion effect alters relative ground-state energies and the relative positions of ground- and transition-state energies. The RSSF spectra and SWSF time courses show that the turnover of indole is significantly reduced in the absence of either $Na^+$ or $K^+$. The α-aminoacrylate Schiff base species, E(A-A), is in a less active state in the absence of monovalent metal ions. $Na^+$ decreases the steady-state rate of IGP cleavage (the α-reaction) to about 30% of the value obtained in the absence of metal ions. Steady-state investigations show that in the absence of monovalent metal ions the α- and $\alpha\beta$-reactions have the same activity. $Na^+$ binding gives a 30-fold stimulation of the α-reaction when the $\beta$-site is in the E(A-A) form. This study demonstrates that the presence of saturating amounts of monovalent metal ions is an important element both for catalysis at the $\beta$-site and for the allosteric linkage between the α- and $\beta$-sites in the bienzyme complex. Theoretical models that describe the monovalent metal ion effect are discussed and tested with the help of computer simulation.

Tryptophan synthase from *Salmonella typhimurium* is a bienzyme complex that catalyzes the final two steps in the biosynthesis of tryptophan (Yanofsky & Crawford, 1972; Miles 1979, 1991). Its subunit composition is tetrameric ($\alpha_2\beta_2$) with subunits arranged in a linear $\alpha\beta\beta\alpha$ order with a total length of ~150 Å (Wilhelm et al., 1982; Lane & Kirschner, 1983; Hyde et al., 1988). The α-subunit catalyzes the cleavage of IGP[1] to G3P and indole (eq 1). The $\beta$-subunit catalyzes the condensation of indole with L-Ser to form L-Trp (eq 2). The overall process, the $\alpha\beta$-reaction, is shown in eq 3.

$$\text{IGP} \rightleftharpoons \text{indole} + \text{G3P} \quad (1)$$

$$\text{indole} + \text{L-Ser} \rightleftharpoons \text{L-Trp} + H_2O \quad (2)$$

$$\text{IGP} + \text{L-Ser} \rightleftharpoons \text{L-Trp} + \text{G3P} + H_2O \quad (3)$$

The active sites of neighboring α- and $\beta$-subunits are separated by about 25−30 Å and connected by a tunnel (Hyde et al., 1988; Hyde & Miles, 1990). The common intermediate indole is preferentially transferred from the α-site to the $\beta$-site by a channeling mechanism involving the interconnecting tunnel (Dunn et al., 1987a,b, 1990, 1991; Lane & Kirschner, 1991; Anderson et al., 1991; Brzovic et al., 1992a). Scheme 1 shows a full outline of the chemical steps involved in the $\alpha\beta$-reaction. A system of reciprocal allosteric interactions exerted through the $\alpha\beta$-subunit interface ensures the coordination of the α- and $\beta$-reactions (Houben & Dunn, 1990; Dunn et al., 1990, 1994; Kirschner et al., 1991; Brzovic et al., 1992a).

A large group of enzymes has been shown to be subject to monovalent metal ion activation or inhibition. A review by Suelter (1970) lists more than 50 enzymes, and an earlier review by Evans and Sorger (1966) lists more than 100 enzymes or enzyme systems affected by monovalent metal ions. Although such a vast number of enzymes show monovalent cation activation, until very recently there has been no detailed information on either the nature of monovalent metal ion-binding sites or the mechanism of action of these monovalent metal ions. In the past 2 years, X-ray structures defining the monovalent metal ion-binding sites present in four enzymes have been published [Toney et al., 1993, 1995; Antson et al., 1994; Isupov et al., 1994; Larson et al., 1994; see also Woehl and Dunn (1995)]. Peracchi et al. (1994) were the first to show that the tryptophan synthase bienzyme complex from *S. typhimurium* is affected by the interaction of monovalent metal ions at a specific binding

† Supported by NSF Grant MCB-9218901.

* To whom correspondence should be addressed at Department of Biochemistry -015, University of California, Riverside, Riverside, CA 92521-0129.

⊗ Abstract published in *Advance ACS Abstracts,* June 15, 1995.

[1] Abbreviations: PLP, pyridoxal phosphate; L-Ser, L-serine; L-Trp, L-tryptophan; IGP, 3-indole-D-glycerol 3′-phosphate; GP, α-glycerol phosphate; $\alpha_2\beta_2$, native tryptophan synthase from *S. typhimurium*; G3P, glyceraldehyde 3-phosphate; E(A-A), enzyme-bound Schiff base of α-aminoacrylate; E(Q), quinonoidal intermediates formed in the conversion of L-Ser and indole to L-Trp; E(Aex), aldimine intermediates formed between the substrate amino acids and the PLP cofactor; RSSF, rapid-scanning stopped-flow; SWSF, single-wavelength stopped-flow; $1/\tau_n$, apparent first-order rate constant of the $n$th relaxation; $A_n$, amplitude of the $n$th relaxation.

0006-2960/95/0434-9466$09.00/0 

Scheme 1

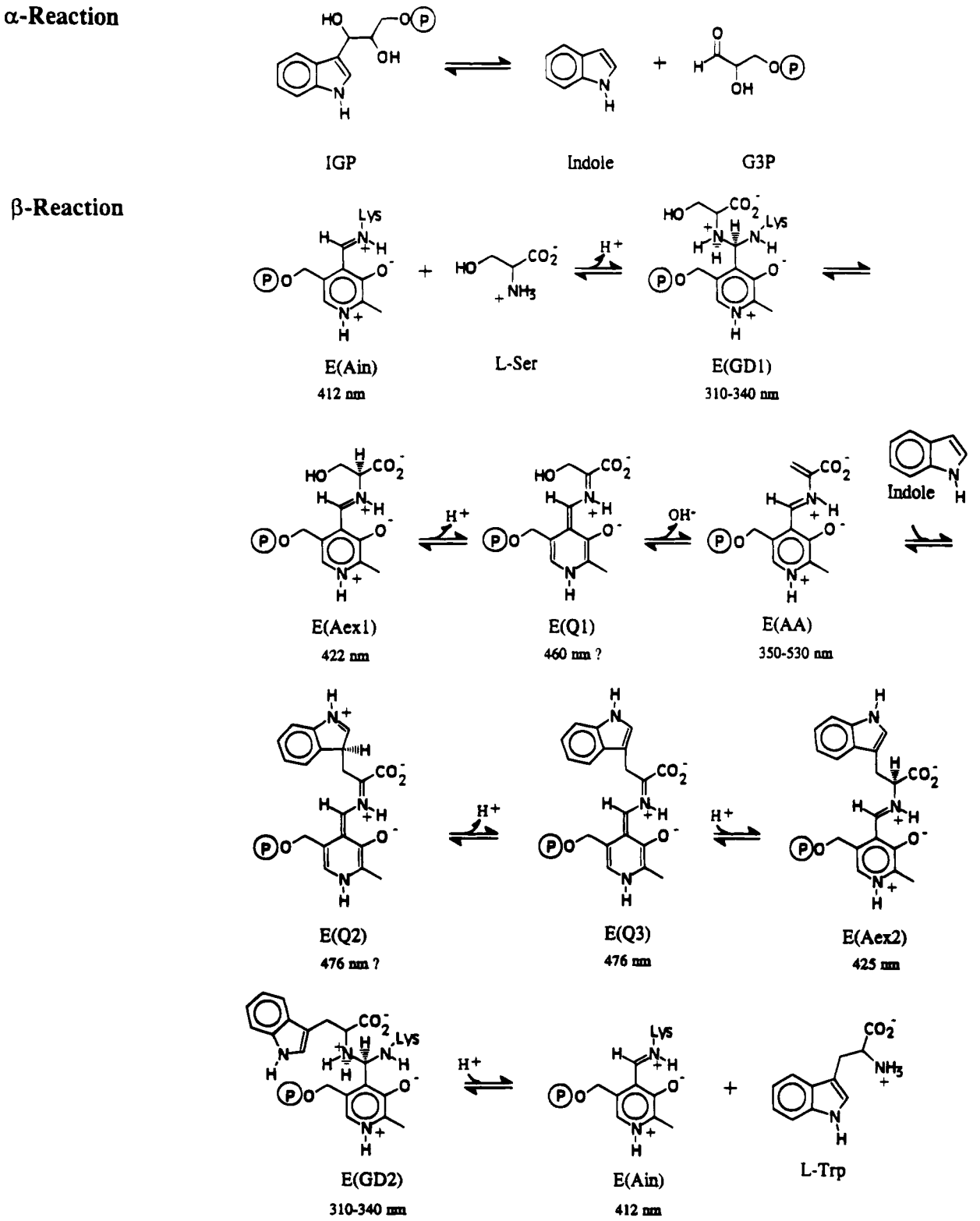


site. They found that monovalent metal ions alter the equilibrium distribution of the $E(Aex_1)$ and E(A-A) species in the reaction of $\alpha_2\beta_2$ with L-Ser [see also Peracchi et al. (1995)]. Even though early work on the $\beta_2$ dimer of tryptophan synthase from *Escherichia coli* had shown changed catalytic behavior in the presence of the monovalent cations $K^+$ and $NH_4^+$ (Hatanaka et al., 1962; Goldberg et al., 1968; Yanofsky & Crawford, 1972; Miles, 1979), the tryptophan synthase $\alpha_2\beta_2$ bienzyme complex was not considered to be monovalent metal ion activated. The details of the tryptophan synthase metal site have not yet been reported.

In an independent study (Weber, 1993; Dunn et al., 1994; Woehl & Dunn, 1995), our laboratory discovered that $Na^+$ and $K^+$ binding strongly influences the reaction of E(A-A) with nucleophiles and strongly activates the turnover rates of the $\beta$- and $\alpha\beta$-reactions and that $Na^+$ and $K^+$ binding is essential for allosteric interactions in the bienzyme complex.

In this investigation of monovalent metal ion effects, a combination of RSSF absorbance and SWSF and fluorescence stopped-flow kinetic techniques have been used to characterize the effects of $Na^+$ and $K^+$ on the individual steps of the $\beta$-reaction and to clarify the mechanism of action. Steady-state measurements have been performed to study the effect of monovalent metal ions on the activity of the $\alpha$-site and on allosteric interactions between subunits. Preliminary accounts of this work have been presented elsewhere (Dunn et al., 1994; Woehl & Dunn, 1995).

## MATERIALS AND METHODS

*Materials.* L-Ser, indole, and D,L-$\alpha$-glycerophosphate were purchased from Sigma. Triethanolamine was purchased from Aldrich as the base and adjusted to pH 7.8 with HCl. IGP was synthesized as previously described (Kawasaki et al., 1987). After lyophylization, the remaining $NH_4^+$ ions were removed using an A-25 column in the $H^+$-form. IGP was loaded onto the column and, after thorough rinsing, eluted with 0.25 M triethanolamine (pH 7.8). Indoline hydrochloride was prepared from the free base by bringing HCl gas onto the surface of a well-stirred mixture of indoline free base dissolved in diethyl ether. Indoline hydrochloride precipitated and was filtered and dried. Metal-free GP was prepared from the disodium salt by repetitively running the solution of the salt over an ion exchange column in the $H^+$-form. Purification of tryptophan synthase from *S. typhimurium* was performed as previously described (Kawasaki et al., 1987; Miles et al., 1987, 1989). The enzyme was dialyzed against metal-free triethanolamine buffer (pH 7.8) to remove monovalent metal ions. This was done prior to usage of the enzyme. The enzyme was stored in Bicine buffer containing monovalent metal ions and PLP.

*UV/Vis Absorbance Measurements.* Static UV/vis absorbance measurements were performed on a Hewlett-Packard 8452A diode array spectrophotometer.

*Turnover Measurements.* Direct photometric assays were used to measure the activity of the $\alpha$-, $\beta$-, and $\alpha\beta$-reactions. The cleavage of IGP to indole and G3P was followed by measuring the decrease in absorbance at 290 nm ($\Delta\epsilon = 1.39$ $mM^{-1}$ $cm^{-1}$; Weischet & Kirschner, 1976b). The conversion of indole to L-Trp was measured by the increase in absorbance at 290 nm ($\Delta\epsilon = 1.89$ $mM^{-1}$ $cm^{-1}$). The conversion of IGP to L-Trp was determined by measuring the increase in absorbance at 290 nm ($\Delta\epsilon = 0.56$ $mM^{-1}$ $cm^{-1}$).

*UV/Vis Titration Studies.* The transient absorbance maximum of the quinonoidal peak in the reaction of E(A-A) with indole was used as a spectrophotometric signal. With increasing concentrations of indole, the transient maximum absorbance at 476 nm increased. Apparent[2] dissociation constants for indole were determined with that method. At saturating concentrations of indole, the transient absorbance maximum increased with increasing monovalent metal ion concentration. The apparent[2] dissociation constants for $Na^+$ and $K^+$ were therefore determined with the same method. SWSF techniques (see below) were used to exactly determine the maximum absorbance attained, and multiple measurements were taken for each concentration point in the titration.

[2] The measured $K_d$ is an apparent $K_d$ since the appearance of the employed signal (quinonoidal peak) involves both binding and chemical reaction.

*Rapid-Scanning and Single-Wavelength Stopped-Flow Measurements.* RSSF and SWSF measurements were performed as previously described (Dunn et al., 1979; Koerber et al., 1983; Drewe & Dunn, 1985, 1986; Brzovic et al., 1990). In each RSSF experiment, a set of 25 scans was collected. The following timing sequences identify the time points for those of the 25 scans shown in the figures. Two different timing sequences were used. Timing sequence 1: 1 = 8.54 ms, 2 = 17.09 ms, 3 = 25.63 ms, 4 = 34.18 ms, 5 = 42.72 ms, 6 = 59.81 ms, 8 = 93.98 ms, 10 = 0.1282 s, 15 = 0.3845 s, 20 = 0.8544 s, 25 = 1.7088 s. Timing sequence 2: 1 = 8.54 ms, 2 = 17.09 ms, 3 = 25.63 ms, 4 = 34.18 ms, 5 = 42.72 ms, 6 = 76.90 ms, 8 = 0.1452 s, 10 = 0.2136 s, 15 = 0.6408 s, 20 = 1.7088 s, 25 = 4.2720 s. Single-wavelength time courses were fit by the Marquardt–Levenberg algorithm to equations of the general form: $A = A_\infty \pm \sum A_n \exp(-t/\tau_n)$.

*Peak-Fitting Analysis of RSSF Spectra.* Single spectra for specific time points of the RSSF spectra set were extracted into separate files and analyzed with the help of a commercial peak-fitting software (PeakFit, Version 3.1; Jandel Scientific). The software applies the Marquardt–Levenberg algorithm to fit a spectrum to a sum of peaks.

The shape of each of the individual peak areas was described using a log normal equation with four independent parameters [as described by Siano and Metzler (1969), Siano (1972), Metzler et al. (1985, 1991), Kallen et al. (1985); see also Houben et al. (1989), Houben and Dunn (1990)]. To correct for light scattering and base line shifts, a curve of the general form $y = ax^{-4} + c$ was used. The parameters of this curve were estimated from absorbance measurements in the 600–800 nm region, where PLP-bound intermediates do not contribute to the absorbance. The E(Aex) species was fit to a single log normal curve with an absorbance maximum at about 423 nm. Extensive studies with quinonoidal intermediates derived from nucleophiles, such as indoline, aniline, or methoxylamine, have shown that tryptophan synthase E(Q) species are fit best by a sum of three log normal peaks (Weber, 1993). For the L-Trp quinonoid, the main peak was centered at 477 nm and the two shoulder peaks were located at 455 and 493 nm. The ratios of the amplitudes of the main peak over the peaks at 455 and 493 nm were 2 and 7.5, respectively. For spectra with a large portion of sites in the E(A-A) form, the E(A-A) peak was fit to two log normals, one centered around 340–350 nm and one low-amplitude peak at about 480 nm. For spectra with a large fraction of the enzyme sites in the E(Aex) state and only traces of E(A-A), the peak at ~480 nm was neglected. The extinction coefficient assumed for the E(Aex) species (10 $mM^{-1}$ $cm^{-1}$) was estimated from the transient maximum of the $E(Aex_1)$ peak reached after rapid mixing of $\alpha_2\beta_2$ with L-Ser. It was assumed that about 90% of the sites were in the E(Aex) state. This $\epsilon$ value is in good agreement with previous estimates (Miles, 1979; Drewe & Dunn, 1985). The quinonoidal extinction coefficient was approximated in a similar way by comparison with the quasi-stable quinonoidal species derived from the indole analogue indoline (Roy et al., 1988; Brzovic et al., 1992b).

## RESULTS

*UV/Vis Static Measurements.* Monovalent metal ions such as $Na^+$, $K^+$, and $Li^+$ influence the UV/vis absorption spectra

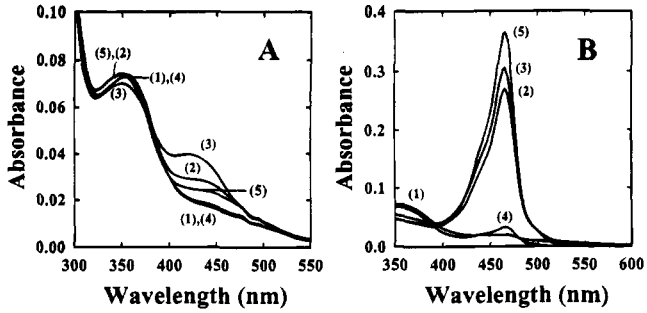


FIGURE 1: (A) UV/vis static absorbance spectra upon reaction of 6 $\mu$M $\alpha_2\beta_2$ with 40 mM L-Ser under the following conditions: without metal ions (1), with 100 mM KCl (2), with 100 mM NaCl (3), with 50 mM metal-free GP (4), or with 50 mM GP and 100 mM NaCl (5). (B) UV/vis quasi-static absorbance spectra obtained after reaction of 6 $\mu$M $\alpha_2\beta_2$ with 40 mM L-Ser and 2 mM indoline under the same set of conditions as in panel A. In contrast to spectra 2, 3, and 5, only trace amounts of the indoline quinonoid are found in the absence of monovalent metal ion, viz. spectra 1 and 4.

of PLP-bound intermediates at the $\beta$-active site (Peracchi et al., 1994; Dunn et al., 1994; Woehl & Dunn, 1995). The effects of $Na^+$ and $K^+$ in the absence and presence of GP on the equilibrium mixture of intermediates obtained in the reaction of L-Ser with enzyme at pH 7.8 and 25 °C are shown in Figure 1A. Under these conditions, these metal ions shift the distribution of intermediates in favor of the $E(Aex_1)$ species. Similar results have been reported by Peracchi et al. (1994). In the presence of monovalent metal ions, this effect is counteracted by the binding of GP to the α-site (trace 5), while without metal ions GP exerts no significant effect on the spectrum (trace 4).

The influence of $Na^+$ and $K^+$ on the quasi-equilibrium mixture of intermediates resulting from the reaction of L-Ser and indoline with the enzyme is shown in Figure 1B. Previous studies have shown that indoline reacts rapidly with E(A-A) (in the presence of $Na^+$ or $K^+$) to give a quasi-stable quinonoidal species that only slowly is converted to the new amino acid, dihydroiso-L-tryptophan (Roy et al., 1988; Brzovic et al., 1992b). The spectra presented in Figure 1B establish that the distribution of species is strongly shifted in favor of the indoline quinonoid by monovalent metal ions. GP, in the absence or presence of metal ions, only weakly perturbs the distribution of species in favor of the quinonoid. The quinonoids derived from other nucleophiles, as, for example, aniline, *O*-methylhydroxylamine, and *N*-methylhydroxylamine, are also similarly influenced by monovalent metal ions. The extent of the effect, however, depends on the nucleophile (data not shown).

*Titrations.* The apparent[2] equilibrium constant for dissociation of indole from the enzyme when premixed with L-Ser was measured in the absence and presence of $Na^+$ ions by observing the transient appearance of E(Q) (data not shown; see Materials and Methods). The calculated dissociation constants are the same within error of the titration (0.1 and 0.09 mM). Titrations were then performed to obtain apparent dissocation constants for $Na^+$ and $K^+$ binding to the enzyme in the presence of saturating L-Ser and indole. The calculated apparent dissociation constants for $K^+$ and $Na^+$ ions are 5 and 1.5 mM, respectively.

*Rapid-Scanning Stopped-Flow Measurements.* RSSF measurements were undertaken to assess the influence of monovalent metal ions on the transient- and steady-state spectra of intermediates in several reactions. Figure 2 shows

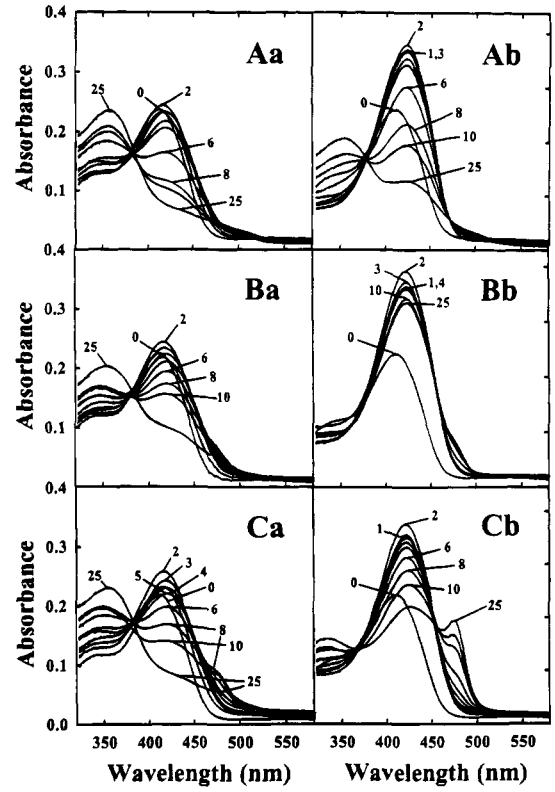


FIGURE 2: RSSF spectra for the reactions of $\alpha_2\beta_2$ with L-Ser (A), L-Ser and indole (B), or L-Ser and IGP (C) shown in the absence (a) and presence (b) of 100 mM NaCl (see Table 1; for SWSF and fluorescence kinetic time courses, see Figures 5 and 7). Concentrations upon mixing were (A) $[\alpha_2\beta_2]$ = 12.2 $\mu$M and [L-Ser] = 40 mM; (B) $[\alpha_2\beta_2]$ = 11.6 $\mu$M, [L-Ser] = 40 mM, and [indole] = 0.5 mM; (C) $[\alpha_2\beta_2]$ = 11.1 $\mu$M, [L-Ser] = 40 mM, and [IGP] = 0.5 mM. Timing sequence 2 was used for panel A and timing sequence 1 was used for panels B and C (see Materials and Methods). In each data set, spectrum 0 is the spectrum of $\alpha_2\beta_2$ measured in the absence of substrates.

RSSF spectra for the reactions of the enzyme with L-Ser (A), L-Ser and indole (B), and L-Ser and IGP (C) in the absence and presence of $Na^+$ ions.

In the reaction of enzyme with 40 mM L-Ser (Figure 2A), the $E(Aex_1)$ species forms rapidly in both the absence (a) or presence (b) of metal ion, and accumulation is complete within the dead time of the experiment (~8 ms). The transient yield of external aldimine, however, is significantly higher in the presence of $Na^+$ ion (compare spectrum 2 of Figure 2Aa with spectrum 2 of Figure 2Ab); and the mixture of intermediates at equilibrium is clearly shifted toward the $E(Aex_1)$ species in the presence of metal ion (compare spectrum 25 in each set from Figure 2Aa,Ab). Peak-fitting analysis of the equilibrium spectra (spectrum 25) showed the following: assuming an estimated extinction coefficient $\epsilon = 10\ mM^{-1}\ cm^{-1}$/site for the $E(Aex_1)$ species [spectrum 2 in the presence of $Na^+$ was taken as 90% $E(Aex_1)$ and the extinction coefficient thus approximated], the percentage of sites in the $E(Aex_1)$ state is estimated as ~11% in the absence and ~24% in the presence of $Na^+$ ions. A summary of the peak fitting results is shown in Table 1.

In the reaction of enzyme with L-Ser and indole (Figure 2B), the transiently formed amount of E(Aex) is again higher in the presence of $Na^+$ ions, and the steady-state spectrum is dramatically changed in the presence of metal ion. The fluorescence stopped-flow data described below show that the external aldimine species is almost exclusively the first

Table 1: Influence of $Na^+$ on the Steady-State or Equilibrium Distribution of $\beta$-Subunit-Bound Intermediates in the $\beta$- and $\alpha\beta$-Reactions (See Figure 2)[a]

| reaction | E(Aex$_1$) (%) | | E(A-A) (%) | | E(Q$_3$) (%) | |
|---|---|---|---|---|---|---|
| | $-Na^+$ | $+Na^+$ | $-Na^+$ | $+Na^+$ | $-Na^+$ | $+Na^+$ |
| | | | $\beta$-Reaction | | | |
| $\alpha_2\beta_2$ + L-Ser | 11 | 24 | 89 | 76 | | |
| $\alpha_2\beta_2$ + (L-Ser + indole) | 19 | 82 | 79 | 15 | 2 | 3 |
| | | | $\alpha\beta$-Reaction | | | |
| $\alpha_2\beta_2$ + (L-Ser + IGP) | 15 | 50 | 83 | 40 | 2 | 10 |

[a] The distribution percentages were estimated from decomposition of the UV/vis spectra as described under the Materials and Methods and Results sections. The distribution percentages were calculated for semiquantitative purposes to provide rough estimates of intermediate distribution with and without NaCl. No detailed error analysis was attempted; the estimated error is 10%.

external aldimine, E(Aex$_1$). Without metal ion, the steady-state spectrum shows the typical features of the E(A-A) species with a strong peak at 355 nm and an absorbance shoulder and tail extending above 500 nm. Peak-fitting analysis indicates the presence of about 19% of sites in the E(Aex$_1$) state. Assuming that the extinction coefficient for the quinonoidal species is about 3.5−4-fold higher than the one for the E(Aex) species, the estimated percentage of sites in the E(Q) state is ~2%. In the presence of $Na^+$ ions, the steady-state spectrum clearly is dominated by the E(Aex$_1$) peak. Peak-fitting analysis shows that ~82% of the sites are in the E(Aex$_1$) state and ~3% of sites in the E(Q) state.

In the reaction of enzyme with L-Ser and IGP (Figure 2C), the transient yield of the E(Aex$_1$) species is again enhanced in the presence of $Na^+$ ions. The most striking difference, however, is found in the steady-state spectra (viz., spectra 25 in a and b). Without $Na^+$ (a), only a small amount of E(Aex$_1$) and a minute amount of quinonoid are present and the spectrum clearly is shaped by a peak at ~355 nm [believed to be characteristic for the E(A-A) species]. In the presence of metal ion (b), the steady-state spectrum (spectrum 25) shows a much smaller peak at ~355 nm and the spectrum is largely comprised of a mixture of E(Q) and E(Aex$_1$) species. Peak-fitting analysis showed the percentage of sites in the E(Aex$_1$) state to be ~15% in the absence and ~50% in the presence of $Na^+$ ions. The estimated percentage of sites in the E(Q) state is ~2% in the absence and ~10% in the presence of metal ion.

Similar changes are found in the $\beta$- and $\alpha\beta$-reactions when the enzyme is premixed with L-Ser (see Figures 3 and 4). One difference, however, is the appearance of a relatively strong transient quinonoidal peak in the presence of monovalent metal ions. This is due to a fast formation of E(Q) from E(A-A) and indole. With the rapid mixing of E(A-A) and IGP, only small amounts of the E(Aex$_1$) and E(Q) species are formed without metal ion (Figure 3A), and the steady-state spectrum is characterized by the peak around 355 nm. In the presence of $Na^+$ ions (Figure 3B), a fairly strong transient quinonoidal peak is formed, and the steady-state spectrum is defined by a mixture of E(Q) and E(Aex1) species.[3] The reaction of E(A-A) with indole was performed in the absence and presence of $Na^+$ ions, $K^+$ ions, and metal-free GP (see Figure 4). Comparing the spectra in the absence and presence of $Na^+$ (Figure 4A,B), there is again a striking difference in the amount of E(Q) and E(Aex$_1$) species formed. Without metal ions (A), only very small amounts of E(Aex$_1$) and E(Q) are formed, whereas in their presence (B), there is a relatively strong transient E(Q) peak and the steady-state spectrum shows mainly the E(Aex$_1$) species. In the presence of $K^+$ ions, the concentration of sites in the E(Q) state is higher in both the steady- and transient-states than in the presence of $Na^+$ ions (data not shown). In the presence of GP but without metal ions (Figure 4C), the steady-state spectrum shows only small amounts of E(Aex$_1$) or E(Q) species; GP does not enhance the amount of E(Q) species at the $\beta$-active site. In the presence of GP and metal ions (Figure 4D), the steady-state spectrum shows increased concentrations of E(Q) and E(Aex$_1$). The distribution of intermediates in the steady state in the presence of metal ions is changed in comparison to the spectra without GP.

[3] The band at 355 nm appears stronger in the steady-state mixture when enzyme and L-Ser are premixed than in Figure 2C due to formation of pyruvate in the syringe with enzyme and L-Ser.

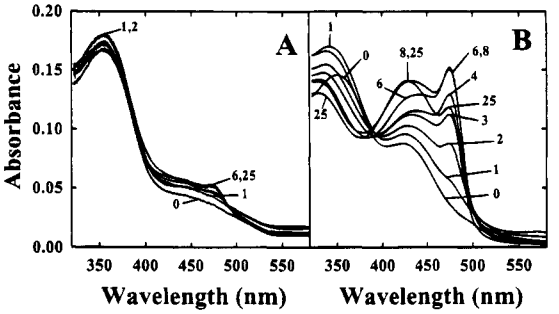


FIGURE 3: RSSF spectra for the reaction of E(A-A) with IGP shown in the absence (A) and presence (B) of 100 mM NaCl. Concentrations upon mixing were [$\alpha_2\beta_2$] = 10 $\mu$M, [L-Ser] = 40 mM, and [IGP] = 0.5 mM. Timing sequence 1 was used (Materials and Methods). In each data set, spectrum 0 is the equilibrium spectrum obtained when $\alpha_2\beta_2$ is reacted with L-Ser in the absence (A) and presence (B) of 100 mM NaCl without IGP. Spectrum 25 in each set is the steady-state spectrum.

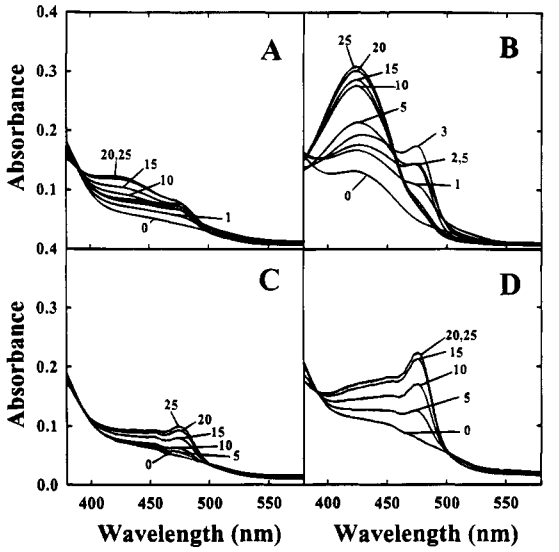


FIGURE 4: RSSF spectra for the reaction of E(A-A) with indole shown in the absence of metal ions (A), with 100 mM NaCl (B), with 50 mM metal-free GP (C), or with 50 mM GP and 100 mM NaCl (D) (see Figure 6 for SWSF time courses). Concentrations upon mixing were [$\alpha_2\beta_2$] = 13.75 $\mu$M, [L-Ser] = 40 mM, and [indole] = 1 mM. Timing sequence 1 was used (Materials and Methods). In each set, spectrum 0 is the spectrum obtained when $\alpha_2\beta_2$ is reacted with L-Ser in the absence of indole while spectrum 25 is the steady-state spectrum.

Table 2: Relaxation Parameters for the Buildup and Decay of the E(Aex$_1$) Species at 420 nm from SWSF Absorbance and Stopped-Flow Fluorescence Measurements (See Figures 5 and 7)[a]

| | | −NaCl | | +NaCl | |
|---|---|---|---|---|---|
| reaction | relaxation/amplitudes | SWSF | fluorescence SF | SWSF | fluorescence SF |
| $\alpha_2\beta_2$ + L-Ser | $1/\tau_1$[c] | | 130 $s^{-1}$ (up)[b] | | 485 $s^{-1}$ (up) |
| | $1/\tau_2$[c] | 20 $s^{-1}$ (down)[b] | 21 $s^{-1}$ (down) | 6 $s^{-1}$ (down) | 7 $s^{-1}$ (down) |
| | $1/\tau_3$[c] | 2.5 $s^{-1}$ (down) | 2.5 $s^{-1}$ (down) | 0.5 $s^{-1}$ (down) | |
| | $A_2/A_3$[e] | 4.5 | 5 | 4.5 | |
| $\alpha_2\beta_2$ + (L-Ser + indole) | $1/\tau_1$[d] | | 135 $s^{-1}$ (up) | | 480 $s^{-1}$ (up) |
| | $1/\tau_2$[d] | 32 $s^{-1}$ (down) | 35 $s^{-1}$ (down) | 30 $s^{-1}$ (down) | 29 $s^{-1}$ (down) |
| | $1/\tau_3$[d] | 2.5 $s^{-1}$ (down) | 2.5 $s^{-1}$ (down) | 2.5 $s^{-1}$ (up) | 3 $s^{-1}$ (up) |
| | $A_2/A_3$[e] | 1.5 | 3 | 5 | 5 |
| $\alpha_2\beta_2$ + (L-Ser + IGP) | $1/\tau_1$[d] | | | | |
| | $1/\tau_2$[d] | 24 $s^{-1}$ (down) | | 17 $s^{-1}$ (down) | |
| | $1/\tau_3$[d] | 2.2 $s^{-1}$ (down) | | | |
| | $A_2/A_3$[e] | 2 | | | |

[a] Standard error is ±15%. [b] The designations (up) and (down) indicate whether the relaxation measured has an increasing or decreasing amplitude. [c] Transient approach to equilibrium. [d] Pre-steady-state relaxation. [e] The first relaxation process is very fast, and a considerable portion of the amplitude is lost in the mixing dead time. Amplitude information for those fast processes is therefore not included in this table.

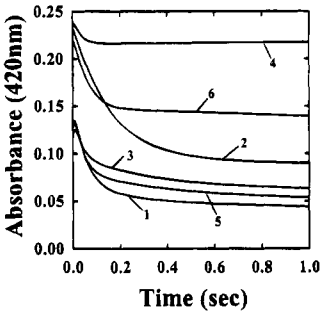


FIGURE 5: SWSF time courses measured at 420 nm shown for the reactions of $\alpha_2\beta_2$ with L-Ser (traces 1 and 2), L-Ser and indole (traces 3 and 4), or L-Ser and IGP (traces 5 and 6) in the absence and presence of 100 mM NaCl (see Table 2). Concentrations upon mixing were 15 $\mu$M $\alpha_2\beta_2$, 40 mM L-Ser, and, where present, 0.5 mM indole or IGP.

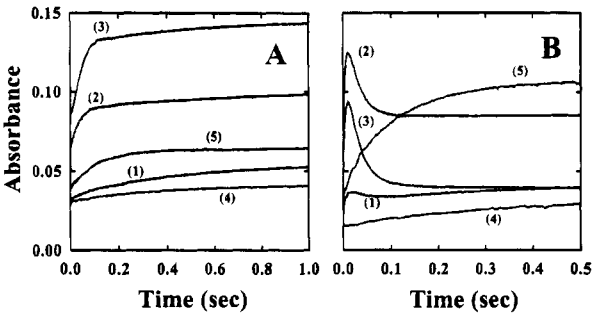


FIGURE 6: SWSF time courses shown for the reaction of E(A-A) with indole under the following conditions: in the absence of metal ions (1), with 100 mM KCl (2), with 100 mM NaCl (3), with 50 mM metal-free GP (4), or with 50 mM GP and 100 mM NaCl (5) (see Table ). Time courses in panels A and B were measured at 420 and 476 nm, respectively. Concentrations upon mixing were [$\alpha_2\beta_2$] = 10 $\mu$M, [L-Ser] = 40 mM, and [indole] = 1 mM.

*Single-Wavelength Stopped-Flow Experiments.* Single-wavelength stopped-flow (SWSF) experiments were performed to investigate the effects of metal ions on relaxation rates. For the reactions of enzyme with L-Ser and with L-Ser and indole, both SWSF absorbance and fluorescence stopped-flow kinetic measurements were performed (see Table 2). The SWSF absorbance measurements for the reaction of enzyme with L-Ser at 420 nm show that the E(Aex$_1$) species (major species absorbing at 420 nm) accumulates within the dead time of the experiment and the decay of E(Aex$_1$) to form E(A-A) is biphasic (Figure 5, traces 1 and 2). Without metal ions, the relaxation rates are 20 and 2.5 $s^{-1}$, respectively, and the ratio of the relaxation amplitudes, $A_1/A_2$, is 4.5. In the presence of $Na^+$ ions, these values drop to 6 and 0.5 $s^{-1}$ and the ratio of amplitudes is unchanged. The stopped-flow fluorescence measurements were performed with a slightly different setup of the observation chamber, so that relaxation constants for the formation of the E(Aex$_1$) species could be determined. The time courses are shown in Figure 7, and the fitted relaxation rate constants are summarized in Table 2. The values for the decay relaxation rate constants were found to be in good agreement with the SWSF absorbance measurements.

Although the signal amplitudes are strongly affected, the rates of decay of E(Aex$_1$) to form E(A-A) in the reaction of enzyme with L-Ser and indole (Figure 5, traces 3 and 4) are not significantly influenced by metal ions. Without metal ions, the relaxation rate constants are 32 and 2.5 $s^{-1}$ with $A_1/A_2$ being 1.5, and both phases occur with decreasing absorbance. In the presence of $Na^+$ ions, the relaxation constants are 30 and 2.5 $s^{-1}$; however, the second phase is increasing rather than decreasing (the increasing phase is only visible in time scales more expanded than the one chosen in Figure 5). The ratio of the relaxation amplitudes for the decreasing and increasing phases, $A_1/A_2$, is 5.

In the reaction of enzyme with L-Ser and IGP to give E(A-A) (Figure 5, traces 5 and 6), the decay of E(Aex$_1$) is also affected; without metal ions, the decay is biphasic with observed rates of 24 and 2.2 $s^{-1}$ and an $A_1/A_2$ of 2; in the presence of $Na^+$, the decay is monophasic with an observed rate of 17 $s^{-1}$. The relaxation rates are summarized in Table 2.

The time courses for the reaction of E(A-A) with indole under various conditions were followed at 420 nm, where E(Aex$_1$) is the main contributor to the absorbance signal, and at 476 nm, where the E(Q) species has its absorbance maximum (see Figure 6 and Table 3). The time courses at 476 nm (Figure 6B) can be described by two phases (one increasing phase, which produces a transient, maximum accumulation of E(Q), and one decreasing phase, where the transient E(Q) peak decays to its steady-state level), both with and without metal ions and in the absence of GP. The time courses in the presence of GP with or without metal ions are described by one increasing phase. The increasing phase without metal ions or GP to give E(Q) is fast (152

Table 3: Relaxation Parameters for the Reaction of E(A-A) with Indole in the Absence and Presence of Effectors from SWSF Measurements at 420 and 476 nm (See Figure 6)[a]

| relaxation/ amplitudes | −GP, −NaCl, −KCl | +KCl | +NaCl | +GP, −NaCl | +GP, +NaCl |
|---|---|---|---|---|---|
| | | 420 nm | | | |
| $1/\tau_1$ (up)[b] | | fast | fast | | |
| $1/\tau_2$ (up) | 60 $s^{-1}$ | 30 $s^{-1}$ | 25 $s^{-1}$ | 2.4 $s^{-1}$ | 8.7 $s^{-1}$ |
| $1/\tau_3$ (up) | 2.3 $s^{-1}$ | 1 $s^{-1}$ | 1.7 $s^{-1}$ | | |
| $A_2/A_3$[c] | 0.3 | 2 | 3 | | |
| | | 476 nm | | | |
| $1/\tau_1$ (up)[b] | 152 $s^{-1}$ | 175 $s^{-1}$ | 207 $s^{-1}$ | | |
| $1/\tau_2$ (down) | 34 $s^{-1}$ | 37 $s^{-1}$ | 42.5 $s^{-1}$ | | |
| $1/\tau_3$ (up) | 3.5 $s^{-1}$ | | | 2 $s^{-1}$ | 9 $s^{-1}$ |
| $A_2/A_3$[c] | 1 | | | | |

[a] Standard error is ±15%. [b] The designations (up) and (down) indicate whether the relaxation measured has an increasing or decreasing amplitude. [c] The first relaxation process is very fast and a considerable portion of the amplitude is lost in the mixing dead time. Amplitude information for those fast processes is therefore not included in this table.

Table 4: Relaxation Parameters for the Reaction of E(A-A) with IGP[a]

| reaction | relaxation/amplitudes | −NaCl | +NaCl |
|---|---|---|---|
| A-A + IGP at 476 nm | $1/\tau_1$ (up)[a] | 20 $s^{-1}$ | 30 $s^{-1}$ |
| | $1/\tau_2$ (up) | 1 $s^{-1}$ | |
| | $1/\tau_3$ (down) | | 15 $s^{-1}$ |
| | $A_1/A_2$, $A_1/A_3$ | 6 | 1.5 |
| A-A + IGP at 420 nm | $1/\tau_1$ (up) | 14 $s^{-1}$ | 15 $s^{-1}$ |

[a] Standard error is ±15%. [b] The designations (up) and (down) indicate whether the relaxation measured has an increasing or decreasing amplitude.

$s^{-1}$), and the rate of this process is slightly increased in the presence of $Na^+$ or $K^+$ ions, 175 and 207 $s^{-1}$, respectively (Figure 6B, traces 1−3). The increasing phase of E(Q) formation is slowed down considerably in the presence of GP (2 $s^{-1}$) (Figure 6B, trace 4). In the presence of GP and metal ions, however, this relaxation rate is increased to 9 $s^{-1}$ (trace 5). The time courses for E(Q) decay to the steady-state level without or with metal ions (traces 1−3) are very similar in rate (around 35−40 $s^{-1}$). The formation of $E(Aex_1)$ at 420 nm measured without GP can be described by the sum of either two (Figure 6A, trace 1) or three (traces 2 and 3) increasing exponentials. In the presence of GP (traces 4 and 5), one increasing exponential is sufficient. The first increasing phase (traces 2 and 3) is only found in the presence of metal ions. It is very fast, and a major portion occurs within the dead time of the experiment. Therefore, no relaxation rate constants could be determined. Without metal ions, this fast phase is absent. The second, increasing phase observed in traces 2 and 3 is slightly slowed in the presence of metal ions from 60 to 25 and 30 $s^{-1}$, respectively. In the presence of GP, the relaxation rate is lowered to 2.4 $s^{-1}$ (trace 4) but increases to 8.7 $s^{-1}$ in the presence of $Na^+$ ions (trace 5).

The reaction of E(A-A) with IGP was also followed at 476 and 420 nm (see Table 4; time courses not shown). Without metal ions, the time course at 476 nm can be described using two increasing exponentials with relaxation rates of 20 and 1 $s^{-1}$. In the presence of $Na^+$, two exponentials, one increasing and one decreasing, are necessary to describe the time course at 476 nm. The increasing and decreasing phases have relaxation rate constants of 30 and 15 $s^{-1}$, respectively. Each time course at 420 nm can be described by a single exponential. The relaxation constants measured without or with $Na^+$ ions are (within error limits) identical, 14 and 15 $s^{-1}$, respectively.

Table 5: Effects of $Na^+$ and $K^+$ on the Activities of the α-, β-, and αβ-Reactions[a]

| reaction | ligand | activity ($s^{-1}$) | relative percent (%) |
|---|---|---|---|
| α-reaction | no metal ions | 0.30 | 100 |
| | $Na^+$ | 0.09 | 30 |
| | $K^+$ | 0.09 | 30 |
| β-reaction[4] | no metal ions | 1.4 | 100 |
| | $Na^+$ | 7 | 500 |
| | $K^+$ | 9 | 640 |
| αβ-reaction | no metal ioins | 0.32 | 100 |
| | $Na^+$ | 3 | 1000 |
| | $K^+$ | 2.6 | 800 |

[a] Standard error is ±10%.

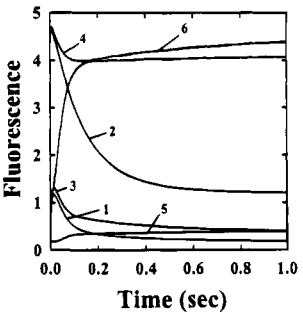


FIGURE 7: Stopped-flow fluorescence time courses for the reaction of $\alpha_2\beta_2$ with L-Ser in the absence and presence of 100 mM NaCl (1 and 2), $\alpha_2\beta_2$ with L-Ser and indole in the absence and presence of 100 mM NaCl (3 and 4), and E(A-A) with indole in the absence and presence of 100 mM NaCl (5 and 6) (see Table 2). Concentrations upon mixing were $[\alpha_2\beta_2]$ = 10 μM, [L-Ser] = 40 mM, and [indole] = 0.5 mM.

*Activity Measurements.* Activity measurements were undertaken for the α-, the β-, and the physiological αβ-reaction (Table 5).[4] Without metal ions, the activities for the α-reaction alone and the αβ-reaction are the same (0.3 $s^{-1}$). In the presence of metal ions, the α-reaction activity (absence of L-Ser) is decreased to 30% of its value without metal ions (0.09 $s^{-1}$). However, the αβ-reaction activity is stimulated 10-fold (3 $s^{-1}$). The β-reaction activity is also stimulated by monovalent metal ions from 1.4 $s^{-1}$ without metal ions to 7 $s^{-1}$ with $Na^+$ and 9 $s^{-1}$ with $K^+$. Steady-state analysis for the αβ-reaction showed a $K_M$ value for IGP of 0.18 mM without metal ions and 0.05 mM in the presence of metal ions. The $V_{max}$ is changed from 0.7 to 3.7 $s^{-1}$.

*Stopped-Flow Fluorescence Measurements.* Fluorescence time courses were measured using an excitation wavelength of 420 nm and observing the first external aldimine species with an emission maximum at 505 nm (see Figure 7). Only $E(Aex_1)$ shows significant fluorescence intensity as reported previously for the *E. coli* enzyme (Goldberg et al., 1968; Lane & Kirschner, 1981). This finding was confirmed for

[4] Activity measurements for the β-reaction were also performed at pH 7, and the effects of the monovalent metal ions at this pH are even greater; $Na^+$ stimulates the β-reaction by 8-fold and $K^+$ by 12-fold under those more physiological conditions. The experiments presented in this paper were carried out at pH 7.8 for purpose of comparison with other publications, since the majority of published research on this enzyme was performed at pH 7.8 or 7.9.

tryptophan synthase from *S. typhimurium*; the reaction of $\alpha_2\beta_2$ with L-Trp shows a quenching of the intrinsic enzyme fluorescence (data not shown). Thus, the time course of the E($Aex_1$) species can be followed separately without interference of the second external aldimine or other species. Therefore, good estimates of the amount of the E($Aex_1$) species can be obtained.

## DISCUSSION

The X-ray structures of three PLP-dependent enzymes, tryptophanase, tyrosine phenol-lyase, and dialkylglycine decarboxylase [see Woehl and Dunn (1994) for a review], and the structure of pyruvate kinase show that in each case the monovalent metal ion-binding site is distinctly separate from the catalytic site, and therefore the metal ion must exert its influence on catalysis indirectly via allosteric ("other site") interactions.

In the case of both tryptophanase (Morino & Snell, 1967; Suelter & Snell, 1977) and tyrosine phenol-lyase (TPL) (Chen & Phillips, 1993), monovalent metal ions activate. For tryptophanase, $K^+$ shifts the position of equilibrium between two conformations of the enzyme, and certain PLP-bound intermediates are preferentially stabilized (e.g., quinonoidal species). The effects of $K^+$ on TPL show similar characteristics. As is the case for tryptophanase, the quinonoidal species is stabilized.

Dialkylglycine decarboxylase also is activated by $K^+$, while $Na^+$ inhibits (Aaslestad & Larson, 1964; Hohenester et al., 1994). The elegant X-ray crystallographic studies of Toney et al. (1993, 1995) have identified two metal ion-binding sites; one of the sites (site 1) prefers $K^+$ as the coordinating metal ion and is located close to the active site, while the site more distant from the active site preferentially binds $Na^+$. When $K^+$ is substituted by $Na^+$ at site 1, the protein structure in the vicinity of site 1 undergoes a conformational change that alters the structure of the catalytic site; the monovalent metal ion coordination sphere changes from six to five coordinate, causing the reorientation of several protein residues, which appears to disrupt substrate binding and catalysis [Toney et al., 1993, 1995; see also Woehl and Dunn (1995)].

These examples of metal ion-activated enzymes show similarities to each other and to tryptophan synthase as to the role of the metal ion and the mechanism of action. The theoretical models discussed below for the tryptophan synthase bienzyme complex might be applied in their basic scheme to the enzymes mentioned above.

*Monovalent Metal Ions Are Cofactors for Tryptophan Synthase.* The finding of monovalent metal ion effects on the equilibrium distribution of species formed in the reaction of L-Ser with $\alpha_2\beta_2$ by Peracchi et al. (1994) [see also Perarchi et al. (1995)] and the results presented in this paper show that the tryptophan synthase bienzyme complex has a specific binding site for monovalent metal ions such as $Na^+$ and $K^+$ and that metal ion binding to this site is critically important both for catalysis and for intersubunit communication of ligand-mediated allosteric effects. At 25 °C, $Na^+$ and $K^+$ cause similar changes in the kinetic behavior of $\alpha_2\beta_2$, a finding that is in contrast to the selectivity for either $Na^+$ (e.g., thrombin) or $K^+$ (DGD, tryptophanase, TPL, or pyruvate kinase) shown by many other monovalent metal ion-activated enzymes.[5] Titration studies for $Na^+$ and $K^+$ establish that, under physiological conditions, the $\alpha_2\beta_2$ metal ion site is well-saturated. Since it is unlikely that the concentration of $Na^+$ or $K^+$ *in vivo* is subject to sudden changes, but is rather a constant, the role of monovalent metal ions in catalysis is more comparable to that of a cofactor than to a regulatory effector. Consequently, the binding of monovalent metal ions is a permanent element of tryptophan synthase catalysis.

*Monovalent Metal Ion Binding Activates Tryptophan Synthase and Is Critical for Subunit Interactions.* The turnover measurements performed for the α- and αβ-reactions demonstrate the importance of monovalent metal ions in the allosteric interactions between the α- and β-subunits. In contrast to what has been reported previously (Kawasaki et al., 1987; Kirschner et al., 1991; Anderson et al., 1991; Brzovic et al., 1992a,b), in the absence of metal ions, the α- and αβ-reactions show the same turnover rates, i.e., the presence of the E(A-A) species at the β-active site does not activate the α-reaction, and this process is rate limiting for the αβ-reaction. In the presence of $Na^+$ ions, the α-reaction is deactivated to 30% of its activity without metal ions. The αβ-reaction, however, is activated by 10-fold in comparison to the activity measured without metal ions. Therefore, in the presence of metal ions, the α-reaction is stimulated 30-fold by the combined effects of metal ion binding and formation of E(A-A) at the β-active site. This result is in agreement with previous studies, where a 30-fold stimulation of the α-reaction by the E(A-A) species was reported (Kawasaki et al., 1987; Brzovic et al., 1992a). Steady-state kinetic studies of the αβ-reaction show that the value of $K_M^{IGP}$ is changed by 3.6-fold from 0.18 mM without metal ions to 0.05 mM in the presence of $Na^+$ ions, and $V_{max}$ is changed by 5-fold from 0.7 to 3.7 $s^{-1}$. Monovalent metal ions help to ensure the efficiency of the bienzyme complex, by slowing down unnecessary cleavage of IGP in the absence of the second substrate, L-Ser, and by increasing the rate of cleavage of IGP when E(A-A) is present at the β-active site.

Monovalent metal ions are essential to the allosteric cross-talk between the α- and β-active sites. The lowered $K_M$ for IGP in the presence of metal ions helps to ensure saturation of the IGP binding site under physiological concentrations of IGP. Monovalent metal ions do not establish that activation by increasing the amount of E(A-A) species. On the contrary, as can be seen in the steady- and transient-state spectra of different stages of the reaction (Figure 2), monovalent metal ions favor the accumulation of the E($Aex_1$) species over the E(A-A) species. This finding is evidence that monovalent metal ion binding triggers a change in the rate-limiting step.

*Metal Ion Effects on the Equilibrium Distribution of Intermediates.* The effects of metal ions on the equilibrium spectrum present after reaction of L-Ser with enzyme or the quasi-equilibrium after the reaction of E(A-A) with indoline (Figure 1) clearly show that the equilibrium distribution of intermediates has been changed. Figure 1A shows that the

[5] In this discussion of monovalent metal ion effects on $\alpha_2\beta_2$, we assume that a single monovalent metal ion site located on each β-subunit is responsible for the herein described effects of $Na^+$ and $K^+$. Nevertheless, the apparent lack of selectivity for these metal ions may imply the existence of two separate sites, one for $Na^+$, the other for $K^+$.

$E(Aex_1)$ species is favored and changes from ~11% or less to ~24% of total $\beta$-sites; Figure 1B shows that the indoline quinonoid is strongly favored in the quasi-equilibrium. Any model describing the metal ion effects therefore must accommodate changes in the relative ground-state energies of the different intermediates along the $\beta$-reaction pathway.

*RSSF and SWSF Characterization of the Metal Ion Effects.* The RSSF studies of the reactions of enzyme with L-Ser, L-Ser and indole, or L-Ser and IGP show an especially interesting set of results (Figure 2). Again, in the reaction of L-Ser with enzyme (A), the equilibrium spectrum consists mainly of E(A-A) species. The presence of $Na^+$ ions shifts this equilibrium slightly toward $E(Aex_1)$. The amount of $E(Aex_1)$ that accumulates transiently is much higher in the presence of metal ions. Without metal ions, the E(Ain) species turns over to the E(A-A) species without significant accumulation of $E(Aex_1)$. However, the proportion of E(A-A) formed is even greater than with metal ions, while the time scale for the reaction is only slightly changed. Any valid model, therefore, must be able to explain the changed transient accumulation of $E(Aex_1)$, the dependence of amplitudes for the transient distribution of intermediates, and the final distribution of intermediates.

In the reaction of L-Ser and indole with enzyme, there is also a much greater accumulation of the $E(Aex_1)$ species. The fluorescence time courses in Figure 7 clearly prove that the accumulating species in the reaction of enzyme with L-Ser and indole is $E(Aex_1)$, not $E(Aex_2)$. The reaction of enzyme with L-Ser and indole shows the same transient yield of the fluorescent $E(Aex_1)$ species as observed in the reaction of enzyme with L-Ser alone. Since in the $\beta$-reaction $E(Aex_1)$ is the only fluorescent external aldimine and the estimated accumulation approaches 90% of sites, the species accumulating in the reaction of enzyme with L-Ser and indole is almost exclusively $E(Aex_1)$. The sets of RSSF spectra obtained without metal ions appear very similar in the absence and presence of indole. Therefore, it can be concluded that the fraction of enzyme sites converted from E(A-A) to other indole-bound species is very small. Apparently, the E(A-A) species has significantly reduced activity, and this results in a quasi-equilibrium resembling the equilibrium after the reaction of L-Ser alone with the enzyme. However, in the presence of metal ions, E(A-A) reacts very rapidly with indole to give E(Q) species which then decay rapidly to a steady-state in which the $E(Aex_1)$ species accumulates. Any model describing these metal ion effects must account for the reduced activity of the E(A-A) species without metal ions. SWSF measurements show that the rate of formation of the $E(Aex_1)$ species is 3.7-fold faster, while the decay of $E(Aex_1)$ is about 3-fold slower in the presence of metal ions.

The reaction of L-Ser and IGP with the enzyme (Figure 2C) shows the same characteristics without metal ions as found in the reactions of L-Ser alone or of L-Ser and indole. The same conclusion can therefore be drawn. There is very little redistribution of the PLP species when E(A-A) is reacted with indole or an indole precursor in the absence of metal ions. The fact that the set of spectra obtained in the presence of metal ions looks so different from the RSSF data for the reaction of L-Ser and indole with the enzyme (compare Figure 2B,C) is probably due to a change in the rate-limiting step, since cleavage of IGP at the $\alpha$-site becomes the slow step under these conditions. The spectra therefore resemble those obtained in the reaction of E(A-A) with indole (Figure 4B); E(A-A) accumulates before IGP has been cleaved. In the reaction of E(A-A) with IGP, the set of RSSF spectra without metal ions shows almost no change (Figure 3A). The steady-state spectrum resembles very much spectrum 0 (enzyme and L-Ser without IGP). E-(A-A) again seems to be in a less active state. In the presence of $Na^+$ ions, there is a significant buildup of $E(Aex_1)$ and E(Q). The reaction of E(A-A) with indole shows similar behavior (Figure 4). Without metal ions, the steady-state spectrum and spectrum 0 (enzyme and L-Ser without indole) are very similar. There is no significant buildup of $E(Aex_1)$ or E(Q). However, in the presence of $Na^+$, E(A-A) is very reactive toward indole and E(Aex1) accumulates.

The SWSF evaluation of the reaction of L-Ser with the enzyme shows a 3-fold decrease in the relaxation rate for the decay of $E(Aex_1)$ in the presence of $Na^+$ (Figure 5). In the presence of indole or IGP, however, $Na^+$ does not have inhibitory effects. In conditions where no indole is present for reaction with E(A-A), the decay of $E(Aex_1)$ to E(A-A) is inhibited. The SWSF measurements for other steps of the reaction show that the relaxation rate behavior is essentially unchanged by $Na^+$ or $K^+$. The relaxation amplitudes, however, are changed significantly. This supports the conclusions drawn from the RSSF spectra, that a redistribution between different enzyme forms with different activities has taken place.

### *Mechanisms for Monovalent Metal Ion Activation of Tryptophan Synthase*

Small ligand effectors, like monovalent metal ions, can exert their effects by binding to the enzyme at loci separate from the catalytic site. Herein, we consider two different principles of action to explain effector-mediated activation/inhibition. A more extensive and detailed discussion of possible mechanisms can be found in Woehl and Dunn (1995). The ligand can play a mainly dynamic, strain-distortion role (Pauling, 1948; Woehl & Dunn, 1995) by stabilizing transition-state versus ground-state energies along the reaction path, thus changing rate constants. In a more structural function, the small ligand stabilizes one of two preexisting conformations of the enzyme, thus changing the equilibrium constant between those conformations (Woehl & Dunn, 1995). On the basis of these two general principles, we here consider two models capable of describing the monovalent metal ion effect. Among a number of different models that were tested, these two most closely reproduced the behavior in the experiment. The models were kept as simple as possible to stress the general principle of action.

*Model 1.* The bound metal ion changes the relative positions of transition- and ground-state energies for the interconversion between different intermediates. This action will result in two different sets of rate constants for metal-bound and metal-free enzyme and, if there are changes in relative ground-state energies as well, a changed distribution of intermediates. Scheme 2b describes the case where metal ion binding is concomitant with the conformational change.

*Model 2.* Alternatively, metal ion binding could change the ground-state energies of preexisting different conformations of the enzyme by binding preferentially to one conformation versus the other. This interaction will result

Scheme 2

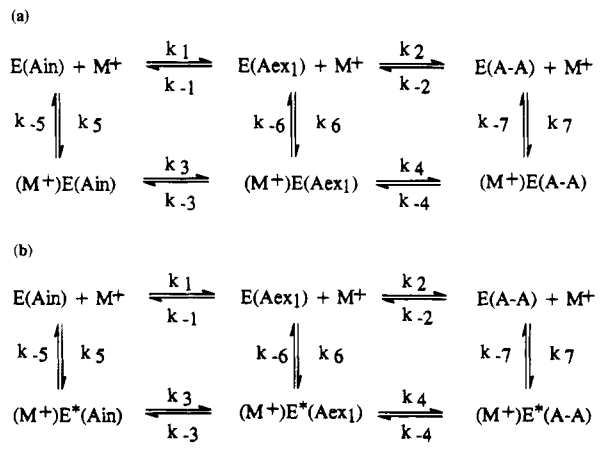


Scheme 3

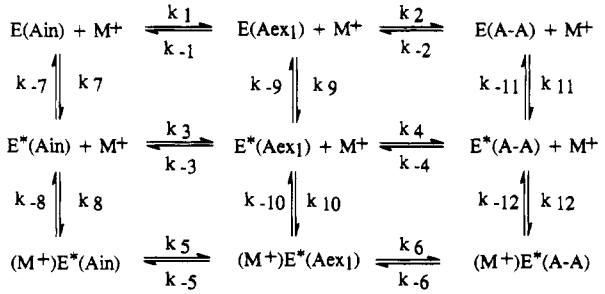


in changed equilibrium constants for the interconversion of conformations. Scheme 3 depicts a mechanism of this type.

More complicated models can be designed; however, they would merely be variations of the basic two models above. To test these two models, simulation studies were undertaken to reproduce the time courses for the reaction of enzyme with L-Ser in the absence and presence of monovalent metal ions. The computational simulation of time courses requires a hypothetical mechanism and the formulation of differential terms for all the species involved. With the help of starting parameters (concentration of reactants and estimated extinction coefficients) and applying the Runge–Kutta algorithm (provided by S. Koerber), the time courses of all the involved intermediates for a certain combination of rate constants can be defined. By a reiterative procedure, solutions to each model that closely replicated the experimental results were found and evaluated. The following four points summarize the criteria of evaluation: (1) The model must show a redistribution of intermediates at equilibrium in the reaction of enzyme with L-Ser. (2) When given the correct starting parameters (concentrations and extinction coefficients of all species involved), the model must reproduce both the metal ion-altered accumulation of the $E(Aex_1)$ species and the transient amplitudes seen in the experiment. (3) The model must be able to describe the changes seen in the relaxation rates for the formation and decay of the $E(Aex_1)$ species. (4) The model must predict the reduced activity of the E(A-A) species toward indole in the absence of monovalent metal ions.

Another question that must be assessed is the influence of possible monovalent metal ion impurities. It was important to find out whether changes in metal ion concentration could cause the rate changes seen in the reaction of enzyme with L-Ser and whether in complete absence of any metal ion impurities the enzyme would be essentially inactive. On the basis of relaxation theory and computer simulation studies, a $Na^+$ concentration dependency of relaxation rates should result in enhanced relaxation rates for both the formation as well as the decay of the $E(Aex_1)$ species. The reverse effects on these two steps observed in the fluorescence as well as the absorption time courses cannot have resulted from contaminating metal ion.

To describe the monovalent metal ion effects, it is therefore necessary to postulate two forms of the enzyme with two different sets of rate constants. These two forms can be either metal-bound and metal-free enzyme, as in model 1, where the metal ion switches the enzyme to a second form via binding interactions or, in model 2, two preexisting conformations of the enzyme and the metal ion binding changes the equilibrium distribution of the two forms. Computer simulation studies show that both models are capable of generating relaxation rates matching the fluorescence time courses as well as producing amplitudes for the total absorbance that match very closely the UV/vis absorption time courses from the experiment. These simulations offer strong support for the hypothesis that two forms of the enzyme with two different sets of rate constants form the basis of the mechanism of action.

Because the $\beta_2$-dimer is activated by monovalent cations, the metal ion-binding site almost certainly is located on the $\beta$-subunit (Hatanaka et al., 1962; Goldberg et al., 1968; Yanofsky & Crawford, 1972; Miles, 1979). The metal ion binding, however, also shows effects on the behavior of the $\alpha$-subunit by strongly influencing the allosteric communication between subunits. It is therefore concluded here that conformational changes, either metal ion-induced, as in model 1, or metal ion-driven through equilibrium shifts, as in model 2, must be an important part of the model to explain the long-range allosteric effects on subunit interactions. The evidence presented in this study establishes that monovalent metal ion binding provides a driving force that selectively assists certain steps in catalysis. We speculate that the monovalent metal ion effects on $\beta$-site catalysis are linked to conformational transitions which drive enzyme-bound intermediates to structures where the bond to be cleaved (or formed) is properly aligned with the PLP ring $\pi$-system [viz., Dunathan's hypothesis, Dunathan (1971)]. The location and characterization of the tryptophan synthase monovalent metal ion site by single-crystal X-ray diffraction would provide new insight into the structural role of monovalent metal ions in tryptophan synthase catalysis and allosteric regulation.

## ACKNOWLEDGMENT

We thank Dr. Steven S. Koerber for providing us with the Runge–Kutta software used to simulate reaction time courses.

## REFERENCES

Aaslestad, H. G., & Larson, A. D. (1964) *J. Bacteriol. 88*, 1296–1303.

Anderson, K. S., Miles, E. W., & Johnson, K. A. (1991) *J. Biol. Chem. 266*, 8020–8033.

Antson, A. A., Dodson, G. G., Wilson, K. S., Pletnev, S. V., Harutyunyan, E. G., & Demidkina, T. V. (1994) in *Biochemistry of Vitamin B6 and PQQ* (Marino, G., Sannia, G., & Bossa, F., Eds.) Birkhäuser Verlag, Basel (in press).

Brzovic, P. S., Holbrook, E. L., Greene, R. C., & Dunn, M. F. (1990) *Biochemistry 29*, 442–451.

Brzovic, P. S., Miles, E. W., & Dunn, M. F. (1991) in *Proceedings of the 8th International Congress on Vitamin B6 and Carbonyl Catalysis* (Wade, H., Soda, K., Fukui, T., & Kagamiyama, H., Eds.) pp 277−279, Pergamon Press, New York.
Brzovic, P. S., Ngo, K., & Dunn, M. F. (1992a) *Biochemistry 31*, 3831−3839.
Brzovic, P. S., Kayastha, A. M., Miles, E. W., & Dunn, M. F. (1992b) *Biochemistry 31*, 1180−1190.
Chen, H., & Phillips, R. S. (1993) *Biochemistry 32*, 11591−11599.
Drewe, W. F., Jr., & Dunn, M. F. (1985) *Biochemistry 24*, 3977−3987.
Drewe, W. F., Jr., & Dunn, M. F. (1986) *Biochemistry 25*, 2494−2501.
Dunathan, H. C. (1971) *Adv. Enzymol. 35*, 79−134.
Dunn, M. F. (1994) in *Handbook on Metal-Ligand Interactions* (Berthon, G., Ed.) (in press).
Dunn, M. F., Bernhard, S. A., Anderson, D., Copeland, A., Morris, R. G., & Roque, J.-P. (1979) *Biochemistry 18*, 2346−2354.
Dunn, M. F., Aguilar, V., Drewe, W. F., Houben, K., Robustell, B., & Roy, M. (1987a) *Indian J. Biochem. Biophys. 24*, 44−51.
Dunn, M. F., Roy, M., Robustell, B., & Aguilar, V. (1987b) in *Proceedings of the 7th International Congress on Chemical and Biological Aspects of Vitamin B6 Catalysis* (Korpela, T., & Christen, P., Eds.) pp 171−181, Birkhäuser Verlag, Basel.
Dunn, M. F., Aguilar, V., Brzovic, P., Drewe, W. R., Houben, K., Leja, C. A., & Roy, M. (1990) *Biochemistry 29*, 8598−8607.
Dunn, M. F.; Brzovic, P. S., Leja, C. A., Houben, K., Roy, M., Aguilar, A., & Drewe, W. F. (1991) *Proceedings of the 8th International Congress on Vitamin B6 and Carbonyl Catalysis* (Wade, H., Soda, K., Fukui, T., & Kagamiyama, H., Eds.) pp 257−264, Pergamon Press, New York.
Dunn, M. F., Brzovic, P. S., Leja, C. A., Pan, P., & Woehl, E. U. (1994) in *Biochemistry of Vitamin B6 and PQQ* (Marino, G., Sannia, G., & Bossa, F., Eds.) pp 119−124, Birkhäuser Verlag, Basel.
Evans, H. J., & Sorger, G. J. (1966) *Annu. Rev. Plant Physiol. 17*, 47−76.
Goldberg, M. E., York, S., & Stryer, L. (1968) *Biochemistry 7*, 3662−3667.
Hatanaka, M., White, E. A., Horibata, K., & Crawford, I. P. (1962) *Arch. Biochem. Biophys. 97*, 596−606.
Hohenester, E., Keller, J. W., & Jansonius, J. N. (1994) *Biochemistry 33*, 13561−13570.
Houben, K. F., & Dunn, M. F. (1990) *Biochemistry 29*, 2421−2429.
Houben, K. F., Kadima, W., Roy, M., & Dunn, M. F. (1989) *Biochemistry 28*, 4140−4147.
Hyde, C. C., & Miles, E. W. (1990) *Biotechnology 8*, 27−32.
Hyde, C. C., Ahmed, S. A., Padlan, E. A., Miles, E. W., & Davies, D. R. (1988) *J. Biol. Chem. 263*, 17857−17871.
Isupov, M. N., Antson, A. A., Dodson, G. G., Dementieva, I. S., Zakomirdina, L. N., & Harutyunyan, E. H. (1994) in *Biochemistry of Vitamin B6 and PQQ* (Marino, G., Sannia, G., & Bossa, F., Eds.) Birkhäuser Verlag, Basel (in press).
Kallen, R. G., Korpela, T., Martell, A. E., Matsushima, Y., Metzler, C. M., Metzler, D. E., Morozov, Y. V., Ralston, I. M., Savin, F. A., Torchinsky, Y. M., & Ueno, H. (1985) in *Transaminases* (Christen, P., & Metzler, D., Eds.) pp 37−109, Wiley and Sons, New York.
Kawasaki, H., Bauerle, R., Zon, G., Ahmed, S., & Miles, E. W. (1987) *J. Biol. Chem. 262*, 10678−10683.
Kirschner, K., Lane, A. N., & Strasser, A. W. M. (1991) *Biochemistry 30*, 472−478.
Koerber, S. C., MacGibbon, A. K. H., Dietrich, H., Zeppezauer, M., & Dunn, M. F. (1983) *Biochemistry 22*, 3424−3431.
Lane, A. N., & Kirschner, K. (1981) *Eur. J. Biochem. 120*, 379−387.
Lane, A. N., & Kirschner, K. (1983) *Eur. J. Biochem. 129*, 561−570.
Lane, A. N., & Kirschner, K. (1991) *Biochemistry 30*, 479−484.
Larson, T. M., Laughlin, L. T., Holden, H. M., Rayment, I., & Reed, G. H. (1994) *Biochemistry 33*, 6301−6309.
Metzler, C. M., Cahill, A. E., Petty, S., Metzler, D. E., & Lang, L. (1985) *Appl. Spectrosc. 39*, 333−339.
Metzler, C. M., Viswanath, R., & Metzler, D. E. (1991) *J. Biol. Chem. 266*, 9374−9381.
Miles, E. W. (1979) *Adv. Enzymol. Relat. Areas Mol. Biol. 49*, 127−186.
Miles, E. W. (1991) *J. Biol. Chem. 266*, 10715−10718.
Miles, E. W., Bauerle, R., & Ahmed, S. A. (1987) *Methods Enzymol. 142*, 398−414.
Miles, E. W., Kawasaki, H., Ahmed, S. A., Morita, H., & Nagata, S. (1989) *J. Biol. Chem. 264*, 6280−6287.
Morino, Y., & Snell, E. E. (1967) *J. Biol. Chem. 242*, 2800−2809.
Pauling, L. (1948) *Am. Sci. 36*, 51.
Peracchi, A., Mozzarelli, A., & Rossi, G. L. (1994) in *Biochemistry of Vitamin B6 and PQQ* (Marino, G., Sannia, G., & Bossa, F., Eds.) Birkhäuser Verlag, Basel (in press).
Peracchi, A., Mozzarelli, A., and Rossi, G. L. (1995) *Biochemistry 34*, 9459−9465.
Roy, M., Keblawi, S., & Dunn, M. F. (1988) *Biochemistry 27*, 6698−6704.
Siano, D. B. (1972) *J. Chem. Ed. 49*, 755−757.
Siano, D. B., & Metzler, C. M. (1969) *J. Chem. Phys. 51*, 1856−1861.
Suelter, C. H. (1970) *Science 168*, 789−795.
Toney, M. D., Hohenester, E., Cowan, S. W., & Jansonius, J. N. (1993) *Science 261*, 756−759.
Toney, M. D., Hohenester, E., Keller, J. W., & Jansonius, J. N. (1995) *J. Mol. Biol. 245*, 151−179.
Weber, E. U. (1993) Masters Thesis, University of California, Riverside, CA.
Weischet, W. O., & Kirschner, K. (1976) *Eur. J. Biochem. 65*, 365−373.
Wells, C. M., & Di Cera, E. (1992) *Biochemistry 31*, 11721−11730.
Wilhelm, P., Pilz, I., Lane, A. N., & Kirschner, K. (1982) *Eur. J. Biochem. 129*, 51−56.
Woehl, E. U., & Dunn, M. F. (1995) *Coord. Chem. Rev.* (in press).
Yanofsky, C., & Crawford, I. P. (1972) in *Enzymes* (Boyer, P. D., Ed.) 3rd ed., Vol. 8, pp 1−31, Academic Press, New York.

BI942958A